Design of a Small Arc-Shaped Antenna Array with High Isolation for Applications of Controlled Reception Pattern Antennas

Gangil Byun, Hosung Choo, and Sunwoo Kim

***Abstract*—This communication proposes the design of an arc-shaped antenna array with high isolation to increase the null depth for controlled reception pattern antenna applications. The array is composed of three identical antennas, and each array element is transformed from a rectangular shape to an arc shape to maximize the distance between antenna edges for isolation improvement. The proposed array is fabricated on a 5.5-inch circular substrate to measure antenna characteristics in a full anechoic chamber and is further evaluated by estimating its null depth in conjunction with the conventional power inversion method. The results prove that the array is suitable to effectively improve the isolation and the null depth at low-elevation angles.**

***Index Terms*—Adaptive antenna array, antenna array, controlled reception pattern antenna (CRPA) array, global positioning system (GPS) antenna, null steering array.**

I. Introduction

A controlled reception pattern antenna (CRPA) array has been developed for a global positioning system (GPS) to mitigate the effects of undesired interferences by steering adaptive pattern nulls [1]. The simplest way of this null steering operation is the power inversion method that determines appropriate array weights for deep nulls to minimize the power of incoming interferences [2]. For effective operation, the CRPA array is required to produce a uniform pattern with high gain, especially at low-elevation angles; this low-elevation gain, however, is easily degraded by mutual coupling in electrically small arrays [3]. Although the isolation characteristics can be improved by incorporating an additional structure [4], developing a different feeding network [5], and increasing the physical distance between array elements [6], these solutions are limited to the improvement of the antenna characteristics without an in-depth concern of the null steering performance.

In this communication, we propose a design of the CRPA array to effectively increase the isolation characteristics of a small array for improved null depth at low-elevation angles. The array is mounted on a 5.5-inch circular ground platform and is composed of three identical antennas. The geometry of each array element is transformed from a conventional rectangular shape to an arc shape to maximize the edge-to-edge distance between array elements for high isolation. A slot is then inserted to more suppress the mutual coupling due to the surface current induced on the ground platform, which results in improved isolation, a more uniform pattern, and higher low-elevation gain. To evaluate the proposed array, it is fabricated on a ceramic substrate, and its matching and radiation characteristics are measured in a full anechoic chamber. Finally, the null depth of the array is estimated by the power inversion method and compared with that of a conventional rectangular-shaped antenna array presented in [7]. The results demonstrate that the null depth can be enhanced at low-elevation angles by adopting the proposed arc-shaped structure.

Manuscript received March 10, 2015; revised September 19, 2015; accepted January 21, 2016. Date of publication February 05, 2016; date of current version April 05, 2016. This work was supported by the Ministry of Science, ICT and Future Planning (MSIP), Korea, under the R&D program supervised by the MSIP.

G. Byun is with the Research Institute of Science and Technology, Hongik University, Seoul 121-791, Korea (e-mail: kylebyun@gmail.com).

H. Choo is with the School of Electronic and Electrical Engineering, Hongik University, Seoul 121-791, Korea (e-mail: hschoo@hongik.ac.kr).

S. Kim is with the Department of Electronics and Computer Engineering, Hanyang University, Seoul 133-791, Korea (e-mail: remero@hanyang.ac.kr).

Color versions of one or more of the figures in this communication are available online at http://ieeexplore.ieee.org.

Digital Object Identifier 10.1109/TAP.2016.2526098

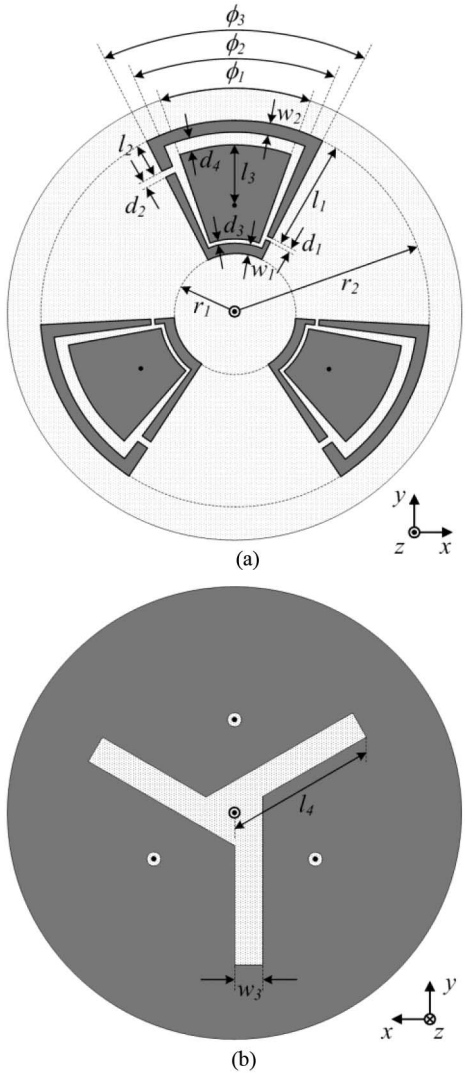

Fig. 1. Geometry of arc-shaped antenna array. (a) Top view. (b) Bottom view.

II. Array Structure and Measurement

Fig. 1 shows the proposed CRPA array that consists of three identical antennas, each of which has a radiating patch and two parasitic strips. The strips have widths w_1 and w_2 and are separated by d_1 and d_2. These separated positions are adjusted by l_1 and l_2, and the distance between the patch and the strips is determined by d_3 and d_4 to adjust the strength of capacitive coupling. This coupling structure induces opposite-direction currents on the strips, thereby enabling flexible axial ratio adjustment for circular polarization [7]. The antenna structure is then transformed to an arc shape, whose radial parameters are r_1 and r_2, and angular parameters are ϕ_1, ϕ_2, and ϕ_3. This arc shape allows the antenna to improve the isolation characteristics because the distance between patch edges, where extremely

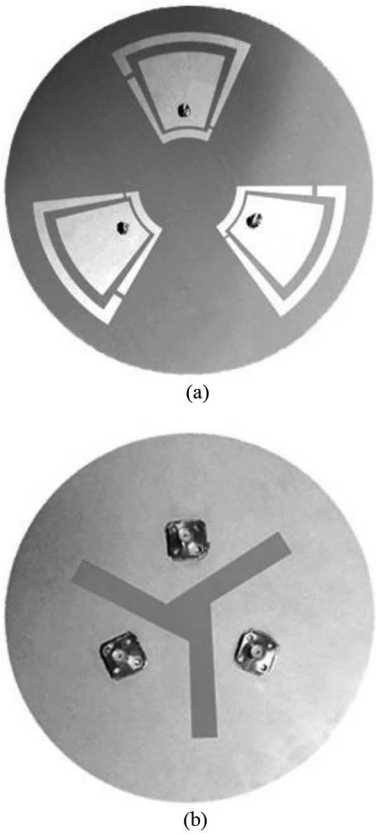

Fig. 2. Photograph of the fabricated array. (a) Top view. (b) Bottom view.

high-density currents are confined, can be maximized. To further improve the isolation, a slot designed with l_4 and w_3 is inserted into the ground plate because it prevents the additional mutual coupling caused by surface currents induced on the ground [8]. Fig. 2 illustrates the proposed array that is fabricated on a 5.5-inch ceramic substrate with a thickness of 7.85 mm ($\varepsilon_r = 10$, $\tan\delta = 0.0035$) [9], and the detailed design values are provided in Table I.

Fig. 3 represents the measured reflection coefficients of the fabricated array at port 1. The measurement is conducted by terminating the other ports with 50-Ω loads, and the measured reflection coefficient is -10.8 dB at 1.57 GHz. Fig. 4 shows the mutual coupling between ports 1 and 2, while port 3 is terminated. To observe the improvement of the isolation characteristics, we compare the mutual coupling of the proposed arc-shaped antenna array with that of the array whose array element has a rectangular shape, as presented in [7]. This rectangular-shaped antenna array is mounted on a circular ground having the same diameter with the ground slot, and the antennas are arranged with an inter-element spacing of 50.1 mm. Although the two arrays have the same inter-element spacing, the mutual coupling can be varied because different patch shapes form different H-field distributions between array elements. The solid line indicates the measured results of the arc-shaped antenna array; the dashed and dotted lines are simulated results of the arc-shaped and rectangular-shaped antenna arrays, respectively. The coupling strength was reduced from -15.7 to -18.6 dB by transforming the rectangular patch to the arc shape and was further improved by 6.2 dB due to the presence of the ground slot, which results in a significant isolation improvement of 9.1 dB. This increased isolation helps reducing the gain mismatch between array elements, which improves the null steering performance in the CRPA operation.

TABLE I
DESIGN PARAMETERS OF ARC-SHAPED ANTENNA ARRAY

Parameter	Value
r_1	18.6 mm
r_2	59.5 mm
w_1	3.3 mm
w_2	3.7 mm
w_3	9.5 mm
l_1	35.0 mm
l_2	10.6 mm
l_3	23.0 mm
l_4	45.7 mm
d_1	0.8 mm
d_2	1.8 mm
d_3	1.0 mm
d_4	3.9 mm
ϕ_1	38.4°
ϕ_2	45.6°
ϕ_3	54.4°

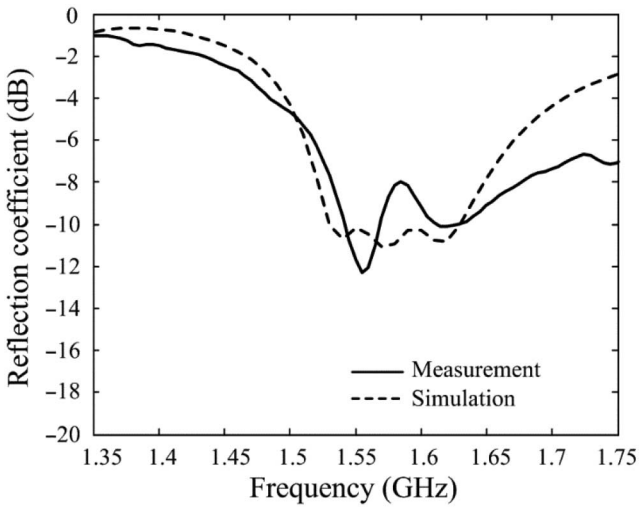

Fig. 3. Reflection coefficient of arc-shaped antenna.

Fig. 5 presents the measured bore-sight gain of the proposed antenna in comparison with the simulation. The solid and dashed lines indicate the measured results for right-hand circular (RHC) and left-hand circular (LHC) polarizations, respectively, which are obtained in a semi-anechoic chamber. The '+' marks represent the gain values measured in a full anechoic chamber, and these data are compared to the simulation indicated by the dotted and dash-dot lines. The measured gains for the RHC polarization are 0.9 and 1.1 dBic at 1.57542 GHz, which are similar to the simulated value of 0.8 dBic. The cross-polarization level of the antenna is 22.7 dB at 1.59 GHz, which implies that the array has circular polarization, as illustrated in Fig. 6. The 3-dB axial ratio bandwidth is from 1.57 to 1.59 GHz, and the minimum value of 1.9 dB is observed at 1.57 GHz.

Fig. 7(a) and (b) illustrates the radiation patterns in the *zx*- and *zy*-planes, respectively. The antenna shows slightly different half-power beamwidths (HPBWs) of 140° and 100° due to the asymmetric antenna geometry and has high cross-polarization characteristics in the

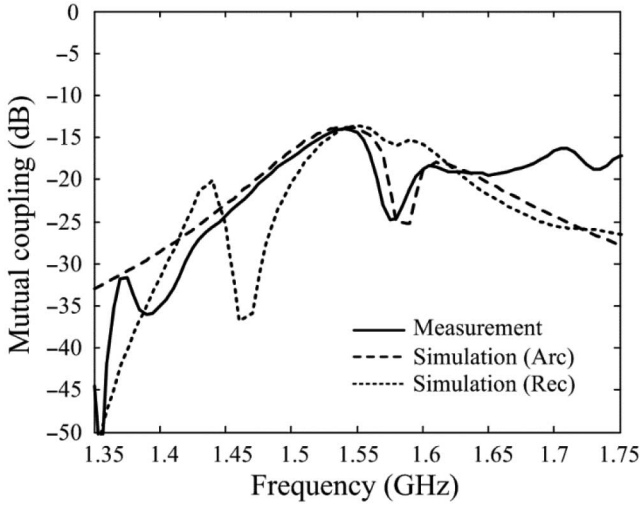

Fig. 4. Mutual coupling between array elements.

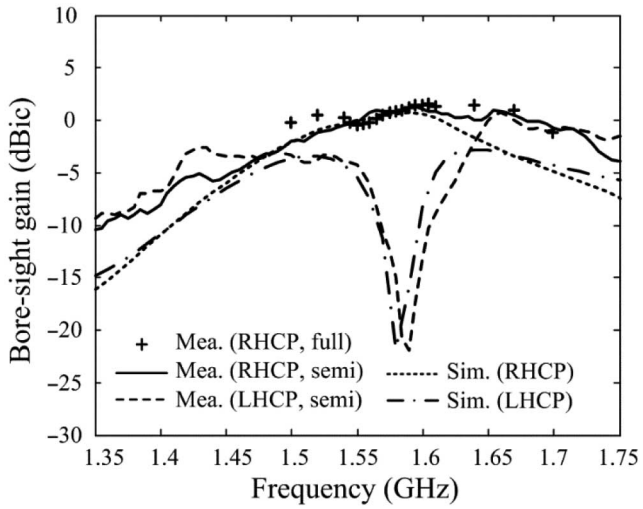

Fig. 5. Bore-sight gain of arc-shaped antenna.

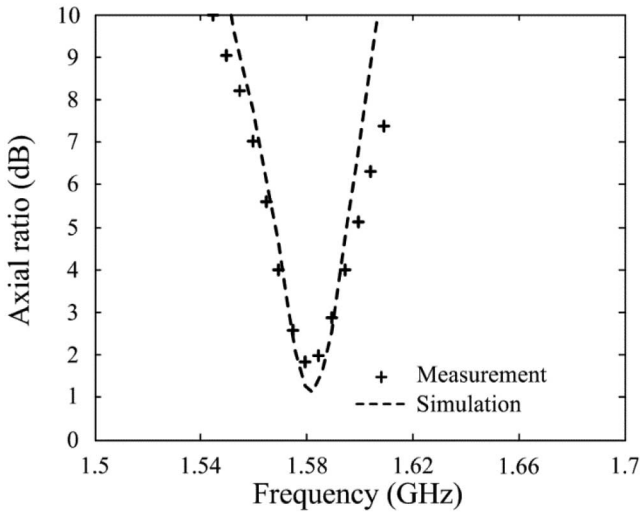

Fig. 6. Axial ratio of arc-shaped antenna.

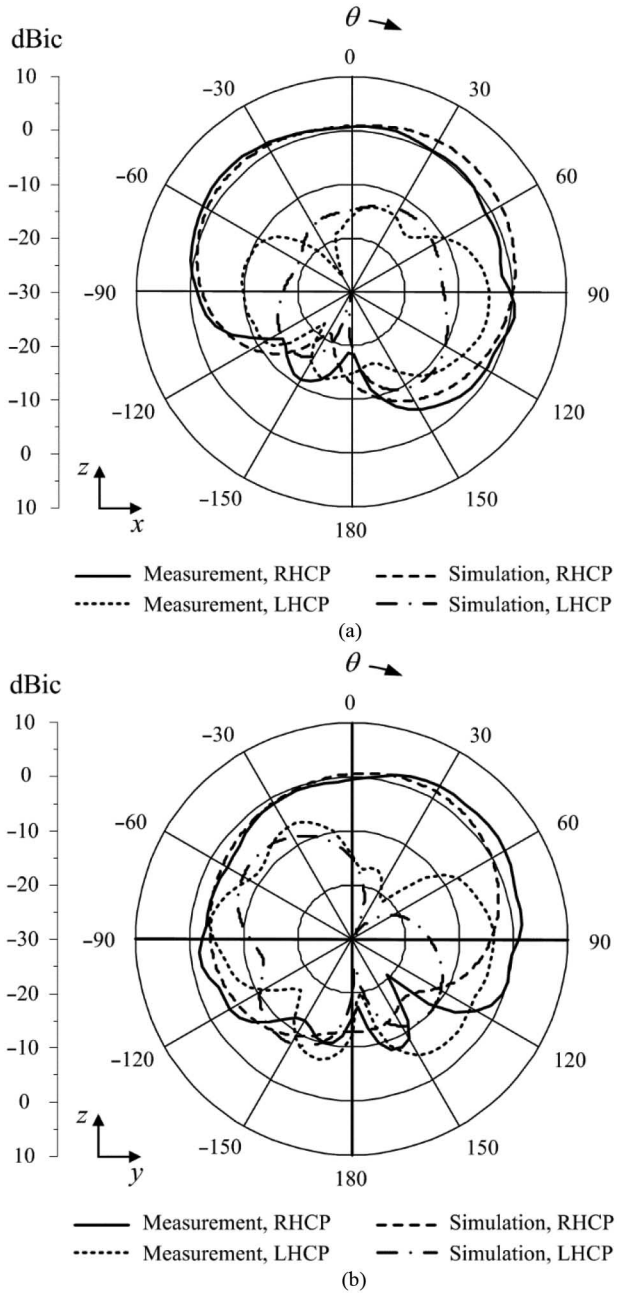

Fig. 7. Radiation patterns of arc-shaped antenna. (a) zx-plane. (b) zy-plane.

θ-direction with the maximum cross-polarization levels of 27.7 and 23.7 dB.

III. CRPA Array Analysis

To demonstrate how the arc-shaped antenna array improves the isolation characteristics, we observe the H-field strength, as illustrated in Fig. 8. The dashed line indicates the H-field strength over a cross-section for the conventional rectangular-shaped antenna array, and the solid line represents that of the proposed array. Each cross-section contains 700 observation points that are placed at intervals of 1 mm to obtain complex H-fields from the simulation, and the simulated values are averaged to estimate the H-field distribution between the array elements. The maximum strength of the rectangular shape is 3.2 dBA/m at $r = 33$ mm, where the closest distance between antenna edges,

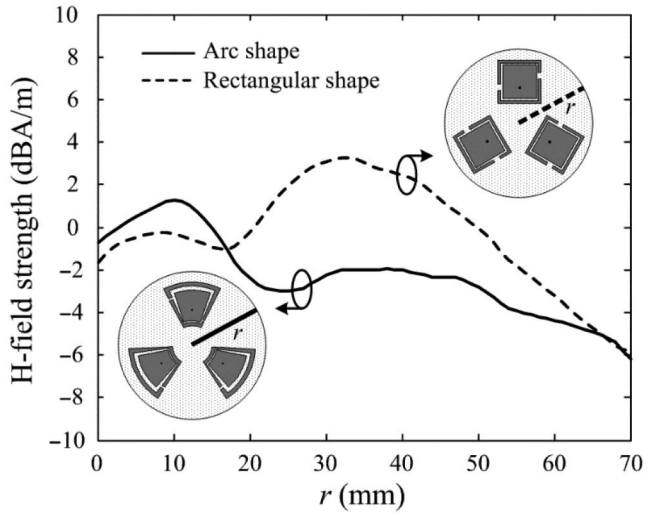

Fig. 8. Comparison of H-field strengths.

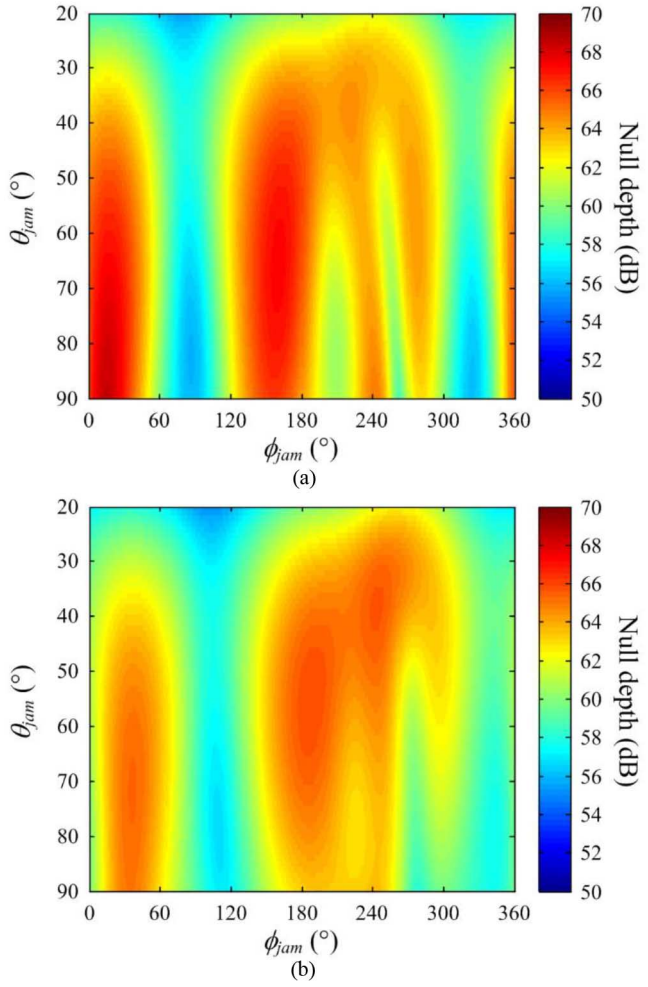

Fig. 9. Comparison of null depths. (a) Arc-shaped antenna array. (b) Rectangular-shaped antenna array.

denoted as the edge-to-edge length, is minimized to 16.6 mm. The isolation can be improved with the proposed array because the field strength is significantly reduced to -2.0 dBA/m due to the maximized edge-to-edge distance of 20.2 mm.

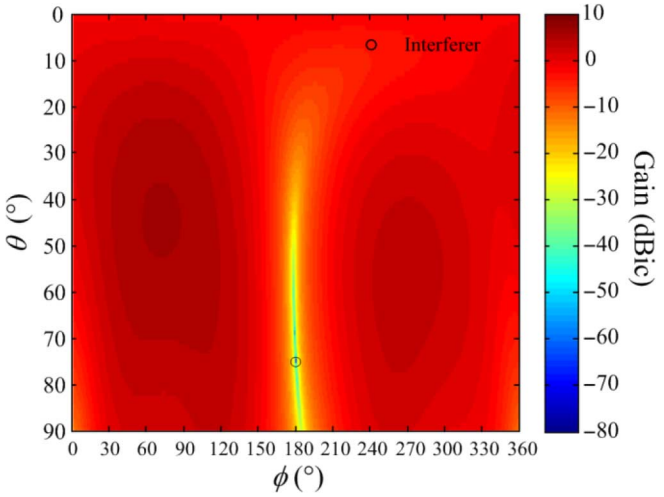

Fig. 10. Null steering pattern of the proposed antenna, when the jammer is placed at $\phi = 180^\circ$ and $\theta = 75^\circ$.

Fig. 9(a) and (b) shows a comparison of null depths between the arc-shaped and the rectangular-shaped antenna arrays. It is assumed that a jamming signal is frequency modulated from 1.45 to 1.65 GHz with a peak power of about -50 dBm and is located in the upper hemisphere from $\theta = 20^\circ$ to $\theta = 90^\circ$. We also assume that the noise floor of the CRPA system is -105 dBm, and the power of GPS signals is about -130 dBm [10]. For a null steering operation, the conventional power inversion method is used to determine appropriate array weights [11]

$$\bar{w}_{opt} = \bar{R}^{-1} \cdot \bar{a} \tag{1}$$

and independent null steering simulations are conducted by varying the direction of jamming signals at intervals of 1°. We define the null depth as given by

$$D_{null} = |G_{opt} - G_{ini}| \tag{2}$$

where G_{opt} indicates the gain value at the jammer direction with $\bar{w}_{opt}$, and G_{ini} represents the value with initial array weights that can be written as

$$\bar{w}_{ini} = \frac{1}{\sqrt{N}} \left[1\angle 0^\circ \;\; 1\angle 0^\circ \;\; 1\angle 0^\circ \right]^T \tag{3}$$

where N denotes the number of array elements. As illustrated in the figure, the improved isolation characteristics of the proposed array increases null depths, especially at low-elevation angles, e.g., the maximum null depth is increased from 65 to 68.5 dB, when the jammer is located at $\theta = 90^\circ$. In addition, the average, minimum, and maximum values are also improved by 0.5, 0.4, and 2.6 dB, respectively, in the range of simulated jammer positions.

Fig. 10 illustrates an example null steering pattern in the upper hemisphere when a jammer is located at $\phi = 180^\circ$ and $\theta = 75^\circ$. We can verify that the proposed antenna is capable of forming a sharp and deep null with a gain value of -65.3 dB without a significant gain reduction in other directions, which validates that the proposed array is capable of improving the null steering performance for the CRPA operation.

IV. Conclusion

We have investigated the design of the arc-shaped antenna array to increase the isolation characteristics for improved null depth in the

CRPA operation. The array is composed of three identical antennas, and each antenna consists of the radiating patch and parasitic strips to achieve circular polarization. To improve the isolation, the shape of each antenna was transformed from the conventional rectangular shape to the arc shape to maximize the edge-to-edge distance, and the ground slot was inserted for further improvement. The proposed array was fabricated, and its antenna characteristics were measured in a full anechoic chamber. The array showed that the reflection coefficient is -10.8 dB, and the bore-sight gain is 1.1 dBic. The axial ratio bandwidth is 16 MHz with the minimum value of 1.9 dB, and the HPBW is greater than 100°. The mutual coupling strength was improved by 9.1 dB compared to the rectangular-shaped antenna array due to the increased edge-to-edge distance, and the null depth was improved by 3.5 dB in the azimuth direction. The results demonstrate that the proposed array is suitable to increase the null depth at low-elevation angles with improved isolation characteristics.

REFERENCES

[1] R. Fante and J. J. Vaccaro, "Wideband cancellation of interference in a GPS receive array," *IEEE Trans. Aerosp. Electron. Syst.*, vol. 36, no. 2, pp. 549–564, Apr. 2000.

[2] O. L. Frost III, "An algorithm for linearly constrained adaptive array processing," *Proc. IEEE*, vol. 60, no. 8, pp. 926–935, Aug. 1972.

[3] Y. Zhou, C. C. Chen, and J. L. Volakis, "Single-fed circularly polarized antenna element with reduced coupling for GPS arrays," *IEEE Trans. Antennas Propag.*, vol. 56, no. 5, pp. 1469–1472, May 2008.

[4] R. O. Ouedraogo, E. J. Rothwell, A. R. Diaz, and K. Fuchi, "Miniaturization of patch antennas using a metamaterial-inspired technique," *IEEE Trans. Antennas Propag.*, vol. 60, no. 5, pp. 2175–2182, May 2012.

[5] G. Byun, S. Kim, and H. Choo, "Design of a dual-band GPS antenna using a coupled feeding structure for high isolation in a small array," *Microw. Opt. Technol. Lett.*, vol. 56, no. 2, pp. 359–361, Feb. 2014.

[6] R. B. Waterhouse, "Small microstrip patch antenna," *Electron. Lett.*, vol. 31, no. 8, pp. 604–605, Apr. 1995.

[7] G. Byun and H. Choo, "Antenna polarization adjustment for microstrip patch antenna using parasitic elements," *Electron. Lett.*, vol. 51, no. 14, pp. 1046–1048, Jul. 2015.

[8] S. Zhang, S. N. Khan, and S. He, "Reducing mutual coupling for an extremely closely-packed tunable dual-element PIFA array through a resonant slot antenna formed in-between," *IEEE Trans. Antennas Propag.*, vol. 58, no. 8, pp. 2771–2776, Aug. 2010.

[9] *CER-10 Data Sheet*, Taconic, Petersburgh, NY, USA, 2005 [Online]. Available: http://www.taconic-add.com/pdf/cer10.pdf

[10] K. Borre, D. M. Akos, N. Bertelsen, P. Rinder, and S. H. Jensen, *A Software-Defined GPS and Galileo Receiver*. Boston, MA, USA: Bitkhauser, 2007.

[11] R.T. Compton Jr., "The power-inversion adaptive array: Concept and performance," *IEEE Trans. Aerosp. Electron. Syst.*, vol. AES-15, no. 6, pp. 803–814, Nov. 1979.

A Frequency-Independent Method for Computing the Physical Optics-Based Electromagnetic Fields Scattered From a Hyperbolic Surface

Yu Mao Wu, Weng Cho Chew, Ya-Qiu Jin, Li Jun Jiang, Hongxia Ye, and Wei E. I. Sha

***Abstract*—In this communication, we propose a frequency-independent approach, the numerical steepest descent path (NSDP) method, for computing the physical optics scattered electromagnetic field on the quadratic hyperbolic surface. Due to the highly oscillatory nature of the physical optics integral, the proposed method relies on deforming the integration path of the integral into the NSDP on the complex plane. Numerical results for the PO-based EM fields from the hyperbolic surface illustrate that the proposed NSDP method is frequency independent in computational cost and error controllable in accuracy.**

***Index Terms*—Critical-point contributions, hyperbolic surface, numerical steepest descent path (NSDP), physical optics.**

I. INTRODUCTION

In electromagnetics (EM), when the product of the external wave number k and the size of the considered object L, i.e., kL ranges from tens to thousands, the analysis of the scattered EM field belongs to the high frequency problem. In this case, the classical physical optics (PO) current approximation [1] has been accepted as an efficient method to calculate the PO-based EM fields scattered from the electrically large scatterers. PO-based EM fields $\mathbf{E}^{(s)}(\mathbf{r})$ from the considered perfect electric conductor scatterers can be represented as three surface integrals [3] of the type

$$I(k,\mathbf{r}) = \int_{\partial\Omega_1} s(\mathbf{r},\mathbf{r}')e^{ikv(\mathbf{r},\mathbf{r}')}dS(\mathbf{r}'). \tag{1}$$

They are called the surface PO integrals, and $\partial\Omega_1$ denotes the surface of the lit region of the considered object, as shown in Fig. 1. The PO integrand in (1) contains the slowly varying amplitude term $s(\mathbf{r},\mathbf{r}')$, and the exponential of the phase function term $e^{ikv(\mathbf{r}')}$. Due to the highly oscillatory phase behavior of the PO integrand, it is quite challenging to calculate the PO integral with frequency-independent workload and error controllable accuracy.

For the calculation of the PO-based EM fields, direct PO solvers [4]–[5] make the computational cost dramatically increase with k. In

Manuscript received December 03, 2014; revised October 02, 2015; accepted January 21, 2016. Date of publication February 05, 2016; date of current version April 05, 2016. This work was supported in part by NSFC 61401103, in part by NSF-SH Grant 14ZR1402400, in part by the talent recruitment under Grant IDH1207001 by Fudan University, in part by the State Key Laboratory of Millimeter Waves Grant K201505, in part by Innovation Fund of PetroChina 2014D-5006-0301, in part by SINOPEC Key Laboratory of Geophysics 33550006-14-FW2099-0034, in part by the Research Grants Council of Hong Kong (GRF 712612 and 711511), in part by US AR120018 contracted through UTAR, and in part by USA NSF CCF Award 1218552.

Y. M. Wu, Y.-Q. Jin, and H. Ye are with the Key Laboratory for Information Science of Electromagnetic Waves (MoE), Fudan University, Shanghai 200433, China.

W. C. Chew is with the Department of Electrical and Computer Engineering, University of Illinois at Urbana-Champaign, Urbana, IL 61801 USA (e-mail: w-chew@uiuc.edu).

L. J. Jiang and W. E. I. Sha are with the Department of Electrical and Electronic Engineering, The University of Hong Kong, Pokfulam, Hong Kong.

Color versions of one or more of the figures in this communication are available online at http://ieeexplore.ieee.org.

Digital Object Identifier 10.1109/TAP.2016.2526065